AIAA JOURNAL Vol. 54, No. 3, March 2016: Author's post-print version (final draft post-refereeing)

Simplified model for flow-heating effect on wave drag and its validation

Erich Schülein*

German Aerospace Center DLR,

Institute of Aerodynamics and Flow Technology,

D-37073 Göttingen, Germany

Simplified prediction method for determination of flow-heating effects on the wave drag of bodies based on the combined analytical-empirical model of the thermal-spike phenomenon is presented. The existing model conceptions addressing certain aspects of this phenomenon were complemented and refined to develop a method suitable for parameter studies. Some reliable experimental and numerical results for the Mach 3 supersonic flow over conically nosed bodies were used as training data to estimate empirically the model parameters. Finally, the method was cross-validated by the different available results for blunt bodies with hemispherical, flat and conical front faces. By this opportunity the ability to predict the influence of some crucial parameters has successfully been demonstrated for the heat input ratio at steady and periodic heating, the normalized heated-wake/filament diameter, the Mach number and the specific heat capacity.

Nomenclature

A, B, C	empirical parameters
c_d	forebody drag coefficient
c_{df}	forebody drag coefficient based on absolute pressure
c_p	specific heat at constant pressure
d	streamtube diameter
d_q	heating source diameter ($d_q = d_1$)
D_{mod}	model diameter
q	specific heat power
K_{pres}	pressure level ratio induced by the unheated flow
K_{sep}	normalized cross-sectional area covered by the recirulation bubble
M	Mach number
p	static pressure
p_{heat}	heating power
p_0	total pressure
p_0'	Pitot pressure
R	radius
Re_D	Reynolds number based on model diameter
s	streamwise coordinate along the model surface
S	cross-sectional area
t_{fil}	traveling time of the heated filament
t_{period}	period time at periodic heating
T	absolute temperature
T_0	total temperature
U	velocity
x	longitudinal coordinate

*Research Scientist, High Speed Configurations Department, erich.schuelein@dlr.de, Senior Member AIAA

δ	boundary layer thickness
η	drag reduction efficiency $\eta = (c_{d0} - c_d)\, 0.5\, \rho_1 U_1^2\, S_{mod}\, U_1 / p_{heat}$
ε	heat input ratio $\varepsilon = q/(c_p T_1)$
ε_0	energy input ratio $\varepsilon_0 = q/(c_p T_0)$
γ	heat capacity ratio
θ	cone half angle
ω	gas rarefaction degree $\omega = \rho_3/\rho_1$
ρ	density

Subscript

∞	free-stream flow conditions
0	total flow conditions, conditions without flow heating
1	flow conditions upstream of the shock wave (zone 1)
2	flow conditions behind the bow shock wave (zone 2)
3	flow conditions behind the heating source (zone 3)
5	flow conditions at the reattachment region (zone 5)
c	conditions at the cone
fil	parameters of the high-temperature filament
q	conditions at the heating source
max	conditions at the efficiency maximum
$maxd$	conditions at the maximum deflection angle
mod	model parameters
sep	recirculation ("separation") bubble parameters
w	wall conditions
wh	wall conditions at flow heating
wo	wall conditions without flow heating
x	based on the longitudinal coordinate
δ	based on boundary layer thickness

I. Introduction

It is meanwhile common knowledge that external flow heating upstream of supersonic blunt bodies is able to reduce their wave drag and to save the thrust required for a supersonic flight.[1–6] Due to the heating of the initially supersonic flow the Mach number and the stagnation pressure are decreased inside the wake behind the heating source. If the deficit of the total pressure upstream of the bow shock wave becomes high enough, a free recirculation bubble in front of the blunt body accompanied by a favorable transformation of the shock wave structure appears (Fig. 1). This phenomenon, called *hot-spike* or *thermal-spike* effect, is most efficient when the heating source cross section is as small as possible.[2–9] According to published results, the drag reduction efficiency (or power ratio) η, defined as the ratio of the saved thrust power to the heating power, is the most recognized dimensionless parameter quantifying this effect. Despite some impressive findings, large quantitative discrepancies in the efficiency indicated in different studies are not always easy to explain.[8] To the author's knowledge, a reliable engineering method for the fast determination of the flow-heating effect on the wave-drag reduction does not exist at the moment. The aim of the present work was to develop and to validate such a method suitable for parameter studies.

The simplified model considered in the present work describes the mechanism of wave drag reduction induced by the hot-spike phenomenon. The sketch of this model is schematically presented in Fig. 2 by the example of the flow over a spherically blunted body. Flow zones in the vicinity of the heating source and over the blunt body are analyzed separately in the next section.

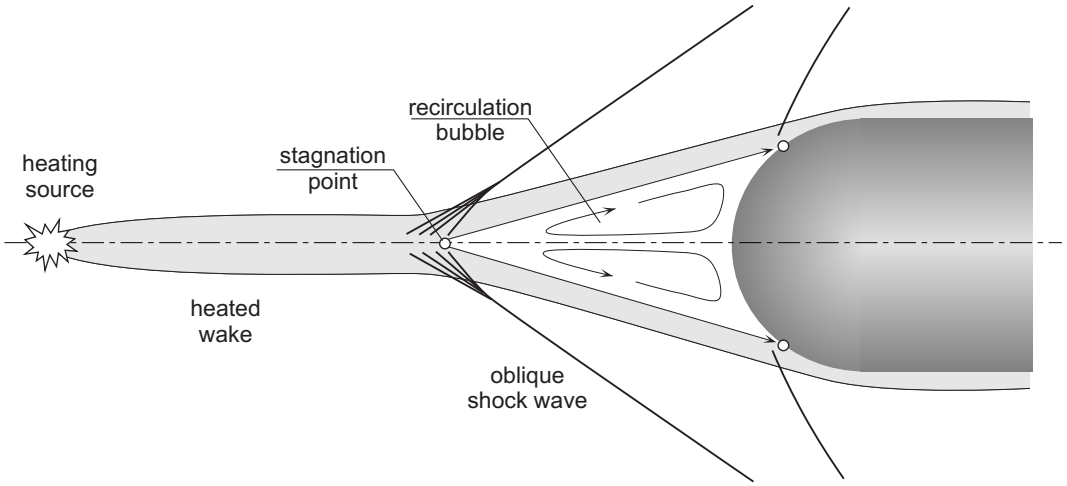

Figure 1. Sketch of the flow field induced upstream of a hemisphere-cylinder body due to the localized flow heating

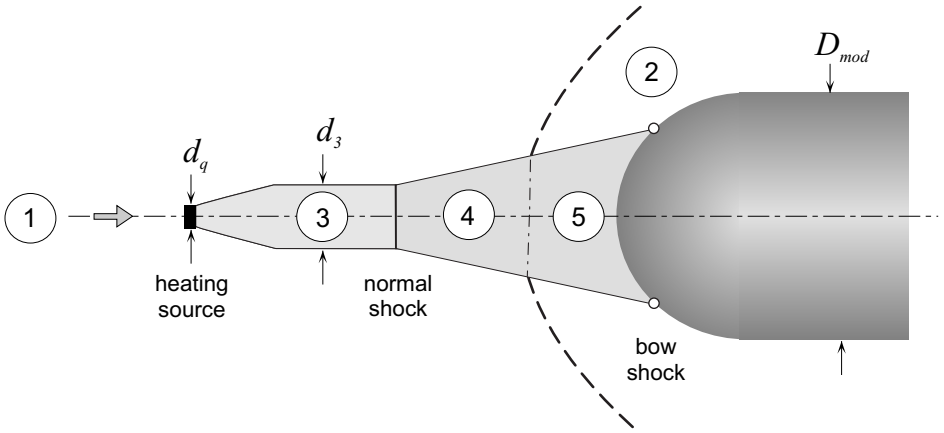

Figure 2. Sketch of the simplified analytical model

II. Model and method description

II.A. Analysis of the flow behind the heating source

At a sufficient distance downstream from the heating source, where the expansion of the heated wake due to the pressure equalization is completed, the flow parameters in the absence of a body can be calculated assuming internal energy addition at constant static pressure conditions. According to OSWATITSCH,[10] the temperatures and densities upstream and downstream of the heating source for the ideal gas conditions at constant specific heats are related to each other as follows:

$$\frac{T_3}{T_1} = \frac{\rho_1}{\rho_3} = 1 + \frac{q}{c_p T_1} = 1 + \varepsilon = \frac{1}{\omega} \tag{1}$$

The subscripts 1 and 3 refer to the zone labels in Fig. 2. Dimensionless parameters ε and ω denoting here the heat input ratio $\varepsilon = q/(c_p T_1)$ and the gas-rarefaction degree $\omega = \rho_3/\rho_1$ are linked to each other and describe the extent of the flow heating alternatively. The specific heat power q introduced to the flow can be determined as $q = p_{heat}/\dot{m}_q = p_{heat}/(\rho_1 U_1 S_q)$, whereby p_{heat} is the heating power, ρ_1 and U_1 are the density and velocity of the undisturbed incoming flow, and S_q is the cross-sectional area of the energy source.

The equation of motion applied to the heated streamtube $\rho u\, du = -dp$ gives a constant-velocity flow at constant pressure, so that the Mach number is changed by increasing sound velocity only

$$\frac{M_3}{M_1} = \sqrt{\frac{T_1}{T_3}} = \sqrt{\frac{1}{1+\varepsilon}}. \tag{2}$$

Hence, the Mach number decreases due to the heating and the resulting flow becomes subsonic when the heating power is high enough. This behavior is additionally supported by the favorable radial extension of the heated streamtube (see Fig. 2, $d_1 = d_q$), taking place in accordance with the density reduction

$$\frac{d_3}{d_1} = \sqrt{\frac{\rho_1}{\rho_3}} = \sqrt{1+\varepsilon} \tag{3}$$

It is important to note that the effect of the thermal flow *chocking*,[11,12] which induces a secondary shock wave upstream of the input zone at high heating rates, is disregarded in this simplified consideration. In this case the stagnation pressure p_{03} in zone 3 can easily be determined from the valid isentropic relations, or alternatively, directly by the relation:[10]

$$ln\frac{p_{03}}{p_{01}} = \frac{\gamma}{\gamma - 1}\left[ln\left(1+\varepsilon_0\right) - ln\left(1+\varepsilon\right)\right], \tag{4}$$

where γ is the ratio of specific heats and ε_0 denotes the energy input ratio $\varepsilon_0 = q/(c_p T_0)$. Finally, the *Pitot* pressure p'_{03} in the heated wake can be calculated on request at locally supersonic flow conditions ($M_3 \geq 1$) by the *Rayleigh supersonic Pitot formula*.[13] Hence, the application of Eqs. 1 - 4 gives a possibility to determine all relevant flow parameters in the heated wake as a function of the heat input ratio ε.

II.B. Analysis of the flow with nonuniform stagnation pressure over a blunt body of revolution

The pioneering analysis of supersonic flows over blunt bodies placed in a region with nonuniform stagnation pressure at nearly constant static pressure (wakes or boundary layers) has been made by MOECKEL.[14] According to his analysis covering two-dimensional and axially symmetric flows, the existence of a localized stagnation-pressure deficit inside a wake upstream of the blunt body (even if velocity near the axis is supersonic) inevitably leads to the formation of a *"dead-air region"* with a free stagnation point ahead of it. This recirculation region is commonly also referred to as *"separation"* or *"front-separation"* zone meaning the flow dividing at the free stagnation point.

The underlying analytical model for the most developed case with a large-scale separation bubble presumes that: 1) the outer border of the separated region is straight, 2) the reattachment of the separated shear layer takes place tangentially to the nose/shoulder of the body, as well as 3) the pressure in the separated region is constant. The most important conclusion of the cited work states that, at given body thickness/diameter D_{mod} and Mach number, a minimum length of the wake (or of the solid-spike) L exists beneath which a steady wedge-/conical-type separation region cannot occur.

Although the effect of the heated wake on the flow ahead of the blunt bodies was not explicitly investigated in the cited work, the most important cornerstones typically for flows with front separation (*solid* or *thermal* spikes, etc.) are definitely at the right place. Above all, the existence of a quasi-steady conical-type separation zone with a lower limit for the length of a solid and thermal spike has been proved in numerous experimental and numerical works and is undisputed. However, the assumptions of the constant pressure inside the separation bubble and the smooth tangential reattachment of the flow to the body seem to be some over-simplifications quite useful only as a first approximation. Based on findings of more recent numerical simulations, the concept of the isobaric recirculation zone is well applicable only to the front part of the separation zone.[4, 15–17] Its rear part, the reattachment region, reveals distinct pressure gradients in most investigated cases and pressure levels which are distinctly higher than expected from the intensity of the separation shock wave.

II.C. Simplified prediction method for flow-heating effect

According to the described model concept, the free recirculation flow ahead of a blunt body occurs when the *Pitot* pressure in the heated wake p'_{03} (or stagnation pressure $p_{03} = p'_{03}$ at locally subsonic flow conditions in the heated wake[a]) becomes equal to or less than the initial static pressure p_2 in the stagnation point region of the body. The pressure level inside the separation zone (see Fig. 2, zones 4 and 5) is assumed to increase from $p_4 = p'_{03}$ at the free stagnation point in zone 4 to a higher level p_5 in zone 5. The reason for this pressure increase is the partial stagnation of the incoming flow due to the non-tangential reattachment of the shear layer to the nose surface, which cannot be analytically calculated. In order to simplify the method, the resulting pressure level in zone 5 is proposed to estimate as a linear composition of the Pitot pressure levels in zones 1 and 3:

$$p_5 = K_{pres}\ p'_{01} + (1 - K_{pres})\ p'_{03} \tag{5}$$

The parameter $K_{pres} = f(\varepsilon)$ is the fraction of the local pressure level assumed to be induced by the unheated flow, which has values between 0 and 1 and should be defined empirically.

For bodies with initially detached bow-shock waves, the separation bubble induced due to heating expands in radial direction as long as the pressure inside it remains lower than the initial local static pressure at the body surface $p_2(s)$, where s is the streamwise coordinate along the surface. It is to be expected that the pressures p_5 and p_2 should be in balance at the junction of the outer border of the recirculation zone and the surface contour (circular markers in Fig. 2). Hence, the wall pressure $p_w(s)$ at the nose part of the body is estimated to be equal to $p_5(\varepsilon)$ inside of zone 5, and equal to $p_2(s)$ outside of it. According to the present method, the initial pressure distribution $p_2(s)$ on the hemispherical model can be estimated as usual by the modified Newtonian theory. For rounded and pointed cones with sonic corners (detached bow-shock waves), the Sin^2-Deficiency Method[18] is supposed to give the best results. The resulting forebody drag can be simply evaluated by integration of the pressure differences acting on the nose surface:

$$c_d = \frac{1}{0.5\rho_1 U_1^2 R_{mod}} \int_0^{R_{mod}} (p_w - p_1) dr \tag{6}$$

Unfortunately, this simple concept for the estimation of the cross-sectional extent of the separation bubble can not be used for slender pointed cones, having initially attached conical bow-shock waves and nominally constant wall pressures at the surface. Similar to the interaction of a flat-plate boundary layer with the shock wave generated by a 2-D compression ramp of finite height[19] (forward-facing step with an inclined front panel), it should be expected that the induced recirculation bubble reaches its full scale when the bow-shock intensity is high enough for the given heated wake profile. For the mentioned 2-D interaction case with a relative thin boundary layer the transformation of the flow topology from the *compression-ramp* (CR) to the *forward-facing-step* (FFS) type occurs very likely when the ramp deflection angle becomes equal to the maximum deflection angle and the bow shock detaches from the nose.[19] If the boundary layer thickness has the same order of magnitude as the ramp height, the transformation to each other is fluid and occurs significantly earlier because each CR-type separation can easily reach *full-scale* extent even at moderate shock intensities.

From this point of view, the heated-wake flow with a CR-type separation bubble is the most common case, while the full-scale separation constitutes only the final state of the flow development and means its

[a]At supersonic flow conditions in the heated wake ($M_3 \geq 1$) a normal shock is assumed to appear upstream of the free recirculation zone (see Fig. 2)

simplification. To extend the proposed approach for more slender bodies with initially attached bow-shock waves, a fraction parameter K_{sep}, quantifying the normalized cross-sectional area of the surface covered by the separation bubble, should be introduced. Using this parameter the flat-rate calculation of the induced forebody drag should be possible regardless of the type of separation bubble as follows:

$$c_d = \frac{K_{sep}(p_{wh} - p_1) + (1 - K_{sep})(p_{wo} - p_1)}{0.5\rho_1 U_1^2} \tag{7}$$

Here, p_{wh} and p_{wo} are the constant pressure levels on the surface of the cone with and without flow heating ($p_{wh} = p_5$, $p_{wo} = p_2$).

III. Model adjustment on the basis of results for pointed cones[9]

To finally adjust the model, the empirical parameters K_{pres} and K_{sep} should be determined on the basis of results available from earlier investigations. In the first step, the parameter K_{pres} should be quantified. In Figure 3 the obtained theoretical predictions for the flow over the conical body with a half angle of 55° are compared with the RANS results.[9] The geometry of the heating source estimated in the cited numerical calculations was used also for the analytical predictions presented. Dashed line ("Theory baseline ($A = 0$)") presents the calculation of the heating effect without correction of the pressure level inside the separation bubble as proposed by Eq. 5. This means that the wall pressure at the nose part of the body is assumed to be equal to the Pitot pressure in the heated wake $p_5 = p_4 = p'_{03}$. The clear difference between this prediction and the proved numerical results confirms the necessity of the more precise surface-pressure estimation.

According to the physical mechanism behind the pressure increase along the separation bubble, the model parameter K_{pres} (see Eq. 5) should be linked to the heat input ratio ε and start to increase as soon as a distinct separation bubble establishes. To describe this behavior, parameter K_{pres} is assumed to be a function of $\Delta\varepsilon = \varepsilon - \varepsilon^*$ which is valid in the range $0 \leq \Delta\varepsilon \leq 4$:

$$K_{pres} = A \; sin\left[\frac{\pi\Delta\varepsilon}{8}\right] \tag{8}$$

where ε^* is the threshold heat input ratio and A is the upper limit for K_{pres}. Outside this range the level of K_{pres} remains constant of $K_{pres} = 0$ at $\Delta\varepsilon \leq 0$ and of $K_{pres} = A$ at $\Delta\varepsilon \geq 4$, correspondingly. The analysis of results presented in Fig. 6 shows that assuming $\varepsilon^* = 1$ as a first approximation the model fits best with numerical results when the parameter A is equal to 0.18 (solid-line solution). The agreement of results for the efficiency level at high heating rates seems to be satisfactory, whereas the drag coefficient predicted shows a small deviations from numerical results, which are fully justifiable taking into account that the proposed method delivers only the wave-drag values.

To improve the prediction at weak and moderate heating rates, the second empirical parameter should be justified. The approach proposed in the present work for a better estimation of the separation-bubble size is based on the empirical scaling law derived earlier in Ref. 20 (see also Ref. 19) for the 2-D compression ramp flows:

$$\frac{L_{sep}}{\delta}\frac{M_1^3}{(p_2/p_{pl})^{3.1}} = f(Re_\delta) = B \tag{9}$$

This relation describes the length of the separation bubble L_{sep} (distance between the separation and reattachment points) normalized by the thickness of the undisturbed boundary layer δ as the function of the Mach number M_1, the Reynolds number Re_δ and the reattachment-shock intensity p_2/p_{pl}. The pressure p_{pl} corresponds to the *plateau* static pressure occurring between the separation and the reattachment shock waves. The parameter $B = f(Re_\delta)$ is assumed to be constant for fixed Reynolds numbers in compression-ramp flows.

Although the Eq. 9 cannot be used directly for axisymmetric heated-wake flows, it offers a good basis for the desired solution. To adapt it consequently, all variables should be replaced by parameters relevant for heated wakes: the intensity of the reattachment shock wave is given here by p_2/p_5 and the heated-wake diameter by d_3. Taking into account that $K_{sep} = S_{sep}/S_{mod} = (d_{sep}/D_{mod})^2$ and $d_{sep} = 2\,L_{sep}\,sin(\theta_{sep})$ the Eq. 9 can be rewritten as follows:

$$\frac{L_{sep}}{d_3} = B\,\frac{(p_2/p_5)^{3.1}}{M_1^3},$$

$$\frac{L_{sep}}{D_{mod}} = B\,\frac{(p_2/p_5)^{3.1}}{M_1^3}\,\frac{d_3}{D_{mod}},$$

$$\sqrt{K_{sep}} = \frac{d_{sep}}{D_{mod}} = 2\,sin(\theta_{sep})\,B\,\frac{(p_2/p_5)^{3.1}}{M_1^3}\,\frac{d_3}{D_{mod}}.$$

Introducing the new variable $C = [2\,sin(\theta_{sep})\,B]^2$ the final equation for K_{sep} is then:

$$K_{sep} = C\left[\frac{(p_2/p_5)^{3.1}}{M_1^3}\,\frac{d_3}{D_{mod}}\right]^2 \tag{10}$$

The valid values for K_{sep} are between 0 and 1. To find a reliable expression for the parameter C the normalized bow-shock intensity $p_2/p_{2,maxd}$ was used as a variable, whereas $p_{2,maxd}$ is the pressure level behind the conical shock wave at the maximum deflection angle for the given Mach number. For pointed cones with attached bow shock waves the pressure levels p_2 and $p_{2,maxd}$ can be determined as usual by solving Taylor-Maccoll equations. The adjustment of the theoretical predictions to the experimental and RANS-computation results[9] for three different pointed cone geometries with $\theta_c = 35°$, 45° and 55° (see Figs. 4-6) delivers the values for the parameter C depended from the normalized bow-shock intensity $p_2/p_{2,maxd}$, which were found to be well approximated by the empirical relation:

$$C = 271.04\left(1 - \frac{p_2}{p_{2,maxd}}\right)^{-0.738} - 270. \tag{11}$$

To use Eq. 11 for bodies with strong shock waves corresponding to $p_2/p_{2,maxd} > 0.92$, this ratio should be set to $p_2/p_{2,maxd} = 0.92$.

As demonstrated in Figs. 4-6, the analytical predictions on the basis of Eqs. 8, 10 and 11 fits well the validation data. Moreover, the agreement of the available data and theoretical predictions could be significantly improved due to following this approach. As can be seen, the more realistic consideration of the separation-bubble size is very advantageous not only for slender cones (Figs. 4 and 5) but also for the cone with initially detached bow shock wave (Fig. 6). A particularly important aspect is the clear and plausible confirmation of the deterioration of efficiency due to the undersized separation bubble observed at weak and moderate heating rates. The maximum efficiency is clearly linked to the threshold heating rate leading first to the full-scale separation ahead of the body. It is important to note that the correlation for the parameter C used is validated hereby for the constant Mach number of $M_1 = 3$ only and should be checked in the future at other flow conditions.

IV. Validation of the method on the basis of published data

IV.A. Steady flow heating for the spherically blunted body at $M_1 = 3$[9]

Figure 7 shows the analytical results (solid line) obtained for the spherically blunted body at Mach 3 in comparison with the own experimental and numerical results obtained earlier.[9] The effect of the heat input ratio ε on the efficiency η as well as on the drag reduction rate $\Delta c_d/c_{d0}$ is shown in this figure as usual. The shape of both functions could be easily reproduced, even though the peculiarities of the flow reattachment on the spherically rounded or angular external corners differs distinctly. The effect of the undersized separation bubble, which covers only the part of the cross-sectional area maximum possible, is visible at $\varepsilon \leq 1$ as sharp efficiency downturn. As mentioned above and was concluded in Ref. 9, the maximum efficiency is achieved when the heating power becomes just enough to induce a full-scale recirculation bubble ahead of the body.

IV.B. Steady energy deposition for the flat-faced cylinder[7, 21]

The available numerical results[7, 21] for the blunt cylinder body at $M_1 = 1.89$ and $\varepsilon = 1.0$ (defined in cited works as $\omega = 0.5$) are the further important test case, used for validation of the proposed simplified theory. The steady heating case is numerically simulated by Norton & Knight (2009)[7] and Anderson & Knight (2011)[21] as an infinitely long high-temperature filament, which corresponds to the heated wake in the zone 3 (see Fig. 2) in accordance with the present analytical model. In Figure 8 the effects of the nondimensional filament (heated wake) diameter d_3/D_{mod} on the efficiency η (top) and the drag reduction ratio $\Delta c_{df}/c_{df0}$ (bottom) for the steady heating case are presented as obtained numerically. The results of both numerical

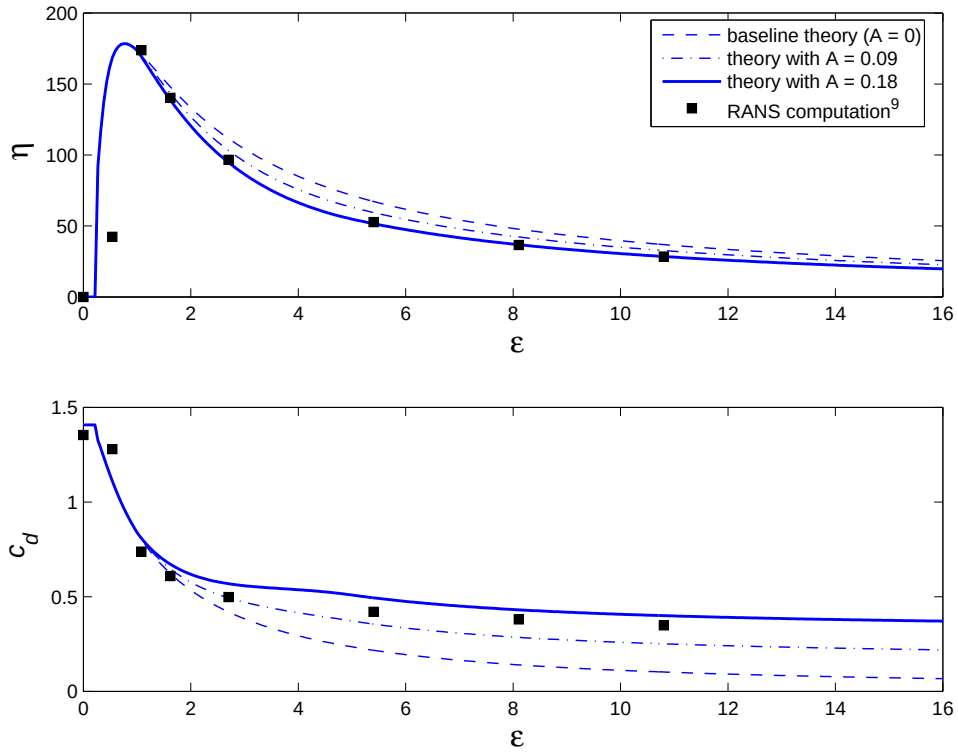

Figure 3. Effect of the heat input ratio on the efficiency and drag reduction level for the cone/cylinder body at $M_1 = 3$ and $Re_D = 1.02 \times 10^6$ ($\theta_c = 55^\circ$, $D_{mod} = 60$mm, $d_q/D_{mod} = 0.077$). Theoretical results are predicted for different A to find the value that best fit the numerical results formerly obtained in Ref. 9.

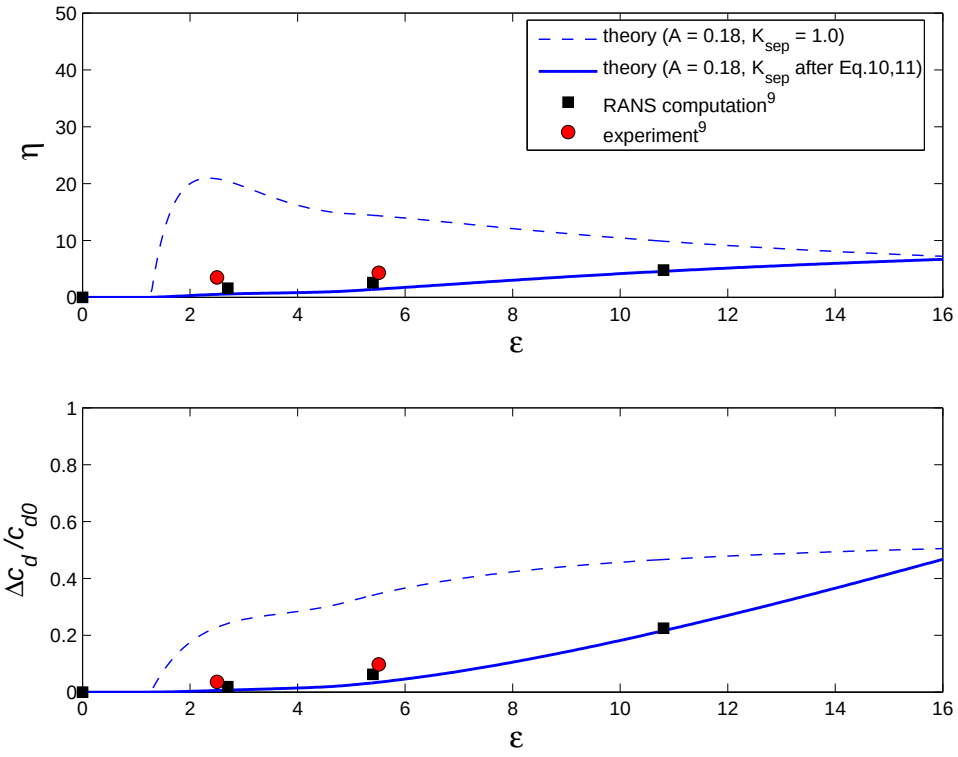

Figure 4. Effect of the heat input ratio on the efficiency and drag reduction level for the cone/cylinder body at $M_1 = 3$ and $Re_D = 1.02 \times 10^6$ ($\theta_c = 35^\circ$, $D_{mod} = 60$mm, $d_q/D_{mod} = 0.077$) with different concepts for K_{sep}

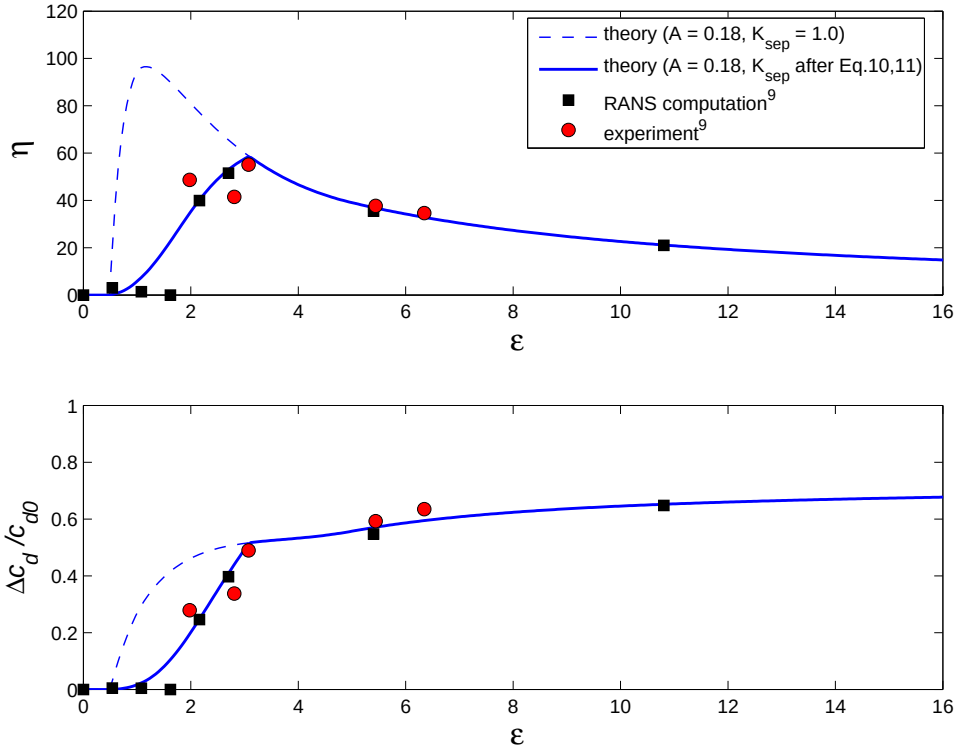

Figure 5. Effect of the heat input ratio on the efficiency and drag reduction level for the cone/cylinder body at $M_1 = 3$ and $Re_D = 1.02 \times 10^6$ ($\theta_c = 45^\circ$, $D_{mod} = 60$mm, $d_q/D_{mod} = 0.077$) with different concepts for K_{sep}

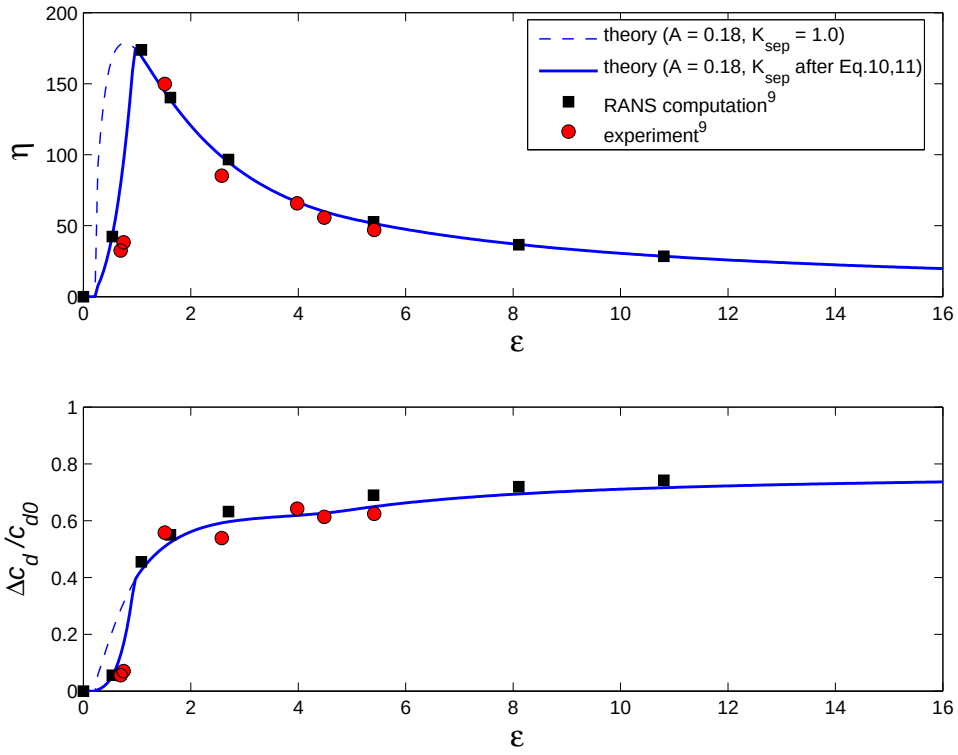

Figure 6. Effect of the heat input ratio on the efficiency and drag reduction level for the cone/cylinder body at $M_1 = 3$ and $Re_D = 1.02 \times 10^6$ ($\theta_c = 55^\circ$, $D_{mod} = 60$mm, $d_q/D_{mod} = 0.077$) with different concepts for K_{sep}

studies could be reproduced here very well on all major points by the method proposed without making use of additional assumptions.

As a side note, contrary to the results demonstrated above, the drag coefficients c_{df} presented in the original works[7,21] and in Figs. 8 and 9 correspond to the integrated absolute wall pressures on the forebody. The drag coefficient c_d discussed in the present paper otherwise is based on the wall-pressure difference $\Delta p = p_w - p_1$ (see e.g. Eq. 6).

IV.C. Average effect of the periodic flow heating for the flat-faced cylinder[21]

The periodic flow heating using longitudinal filaments of limited length at $M_1 = 1.89$ investigated by Anderson & Knight (2011)[21] seems to be also well suited for the analysis via developed simplified method (Fig. 9). The average efficiency and drag reduction ratio are presented here for the flat-faced cylinder over the nondimensional filament-traveling time t_{period}/t_{fil} (in the original work referred as the length ratio L_{period}/D_{mod} at $L_{fil}/D_{mod} = 1$). This normalized time is defined as the ratio of the full period time t_{period} to the filament passing time t_{fil} and is the reciprocal of the duty cycle. Thus, a filament-traveling time of 4 means the existence of a heated filament at the nominally location of the bow shock in 1/4 the time and, correspondingly, its absence in 3/4 the time. To predict this periodic heating effect by the proposed approach the resulting drag coefficient $c_{d,av}$ was estimated as a temporal average value over the full period:

$$c_{d,av} = \frac{t_{fil}}{t_{period}} c_d + (1 - \frac{t_{fil}}{t_{period}}) c_{d0} \tag{12}$$

As can be seen in Fig. 9, the cited numerical results could be reproduced very well by this simplified linear approach, demonstrating that the positive effect of a longitudinal high-temperature filament upstream of the body on the drag reduction lasts only as long as it exists.

IV.D. Average effect of the high-frequency flow heating for different truncated cones[22]

The high-frequency short-pulse flow heating upstream of the truncated cones at $M_1 = 2$ investigated by Sakai (2009)[22] was used for validation purposes as the most challenging test case. Some results obtained in the cited numerical work are presented in Fig. 10, where the average efficiency η and drag reduction ratio $\Delta c_d/c_{d0}$ are presented over the ratio d_{trunc}/D_{mod} for the repetition rate of 100 kHz at a constant energy deposition level of 3 mJ/pulse. According to this work, the truncated cone has a half angle of 30° and the base diameter of 20 mm, while the pulse duration is of 9 ns and the energy deposition is located at $x = 2.5 d_{trunc}$ upstream of the nose.

Contrary to the time-resolved periodic-heating case described above, the high-frequency effect was reproduced in the present work assuming a steady flow heating, taking place correspondingly with the averaged heating power of 300 W. The quasi-steady thermal-spike effect was reported at these conditions in the original work.[22] The treatment of a single heating event for nanosecond-short pulses would go beyond the thermal-spike-model conception, which presumes a longer-lasting heating effect.

The agreement of average results obtained by unsteady Euler simulations[22] and by the method proposed in the present paper seems to be surprisingly well. It is important to note, that demonstrated representation of repetitive flow heating by the steady approach is reliable and adequate if the repetition rate is high enough to induce a quasi-steady recirculation bubble ahead of the body.

IV.E. Study of the Mach number and specific heat capacity effects for a pointed cone

To demonstrate the ability for parameter studies, two different effects, which were not investigated analytically up to now, are presented in Figs. 11 and 12. The first one is the effect of the freestream Mach number on the efficiency and the drag reduction effect predicted for the pointed cone model with $\theta_c = 55°$ (Fig. 11). The maximum efficiency shows a disproportionate increase with the Mach number. Considering the known increase of the wave drag of blunt bodies with the Mach number and the discussed similarity of the thermal- and solid-spike phenomena, this effect seems to be plausible. The next effect demonstrated in Fig. 12 is the impact of different gases on the efficiency and drag reduction effect for the same model configuration at a fixed Mach number of 3. This effect is obviously induced primarily according to the differences in the specific heat capacities c_p of the chosen gases. In the case of a lower c_p, less heating power is needed to reach the critical deficit of stagnation pressure in the heated wake and vice versa (cp. Eq. 4).

IV.F. Shock tube experiments for a rounded cone in air and argon flows[23]

Both effects presented in IV.E seem to explain the reasons for the large experimental discrepancies in the efficiency of the localized heating observed in air and argon flows in Ref. 23. In cited experiments with a rounded cone model ($\theta_c = 60°$, $R_{nose} = 15$mm, $D_{mod} = 60$mm, $L/D_{mod} = 1.167$), an increase of the efficiency from $\eta = 89$ (air flow at Mach 6) up to 463 (argon flow at Mach 9) was demonstrated. According to the present model predictions, the maximum possible efficiency achievable at these test configurations is $\eta_{max} = 637$ for the Mach 6 air flow and even $\eta_{max} = 2249$ for the Mach 9 argon flow (assuming $d_q/D_{mod} = 0.08$). Due to the lack of information regarding the real dimensions of the heating source and the energy losses in the experiment, a direct comparison of the experimental and theoretical results is not possible at the moment.

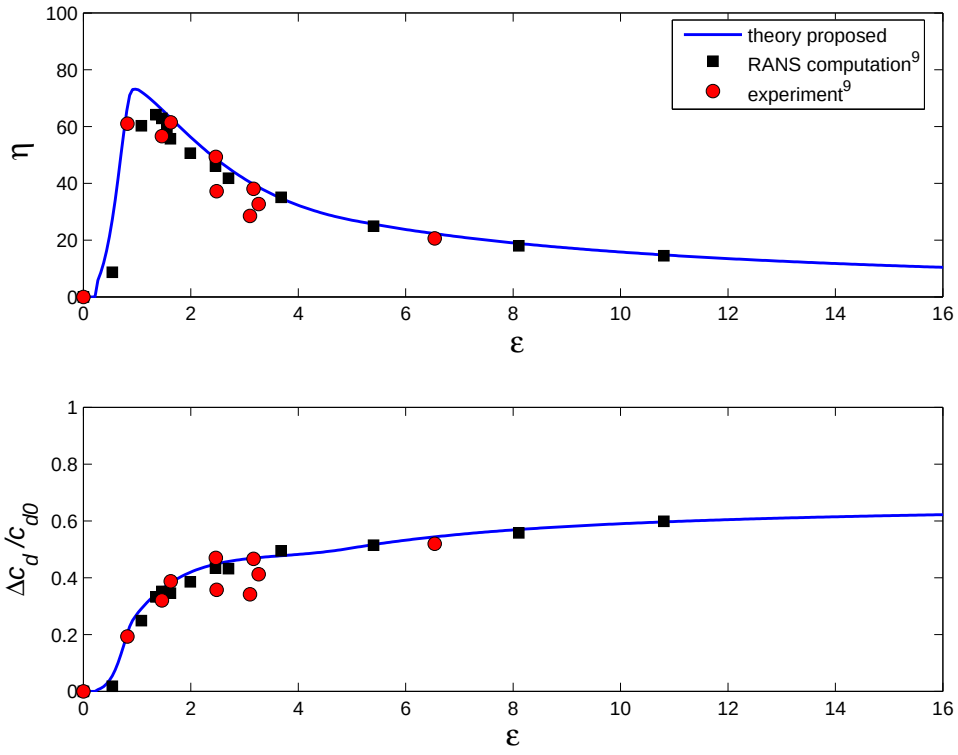

Figure 7. Validation of the simplified theory by results formerly obtained in Ref. 9 for the hemisphere/cylinder body at $M_1 = 3$ and $Re_D = 1.02 \times 10^6$ ($D_{mod} = 60$mm, $L/D_{mod} = 3.67$, $d_q/D_{mod} = 0.077$).

V. Conclusions

A simplified method for predicting the quasi-steady flow heating effect on the wave drag of blunt bodies based on the modeling of the thermal-spike phenomenon is proposed and demonstrated in the present paper. According to the described model concept, two empirical parameters were defined and verified in the present work: 1) coefficient K_{pres}, quantifying the percentage static pressure level induced by the unheated flow underneath the recirculation bubble, and 2) coefficient K_{sep}, being the scale for the cross-sectional area part covered by the separation bubble. Both these parameters were carefully adjusted on the basis of available experimental and numerical results for the Mach 3 supersonic flow over different conically nosed bodies. The found relations for K_{pres} and K_{sep} complement the main analytical model and have a major impact on the demonstrated reliability and accuracy of the prediction method. Finally, the developed method has been successfully validated by some experimental and numerical results for different bodies with hemispherical, flat and conical front faces published in the open literature. The ability to predict analytically the influence of the heat input ratio for steady and periodic flow heating, the normalized filament diameter, the Mach number and the specific heat capacity has been demonstrated in the present work.

The prediction method proposed reproduces the most important results concerning the heating effect on

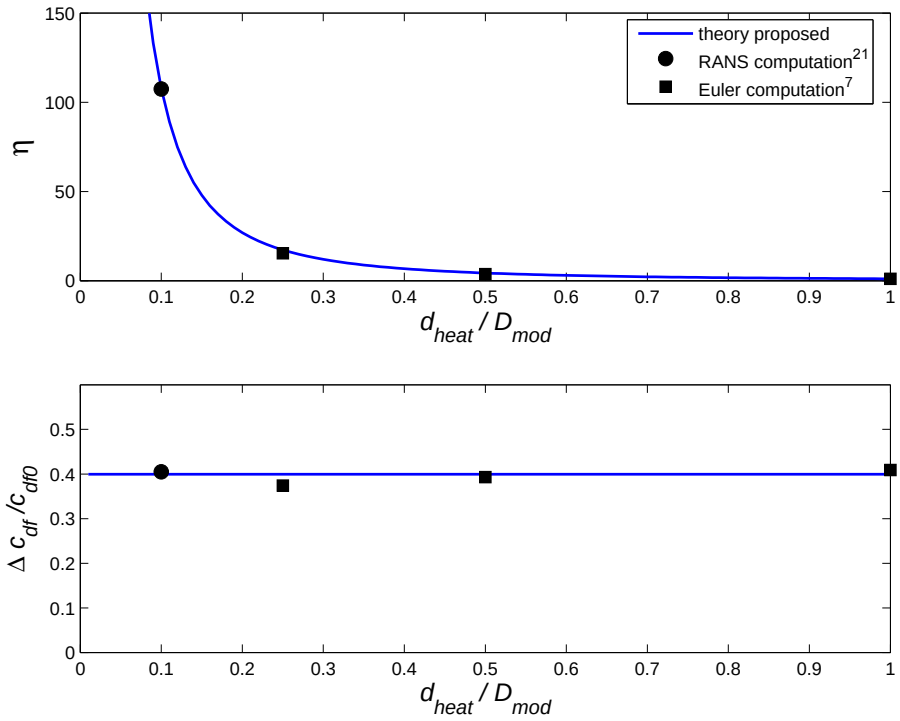

Figure 8. Effects of the relative heated wake diameter d_3/D_{mod} on the efficiency η (top) and drag reduction ratio $\Delta c_{df}/c_{df0}$ (bottom) for the blunt cylinder body at $M_1 = 1.89$ and $\varepsilon = 1.0$, as obtained numerically in Refs. 7, 21

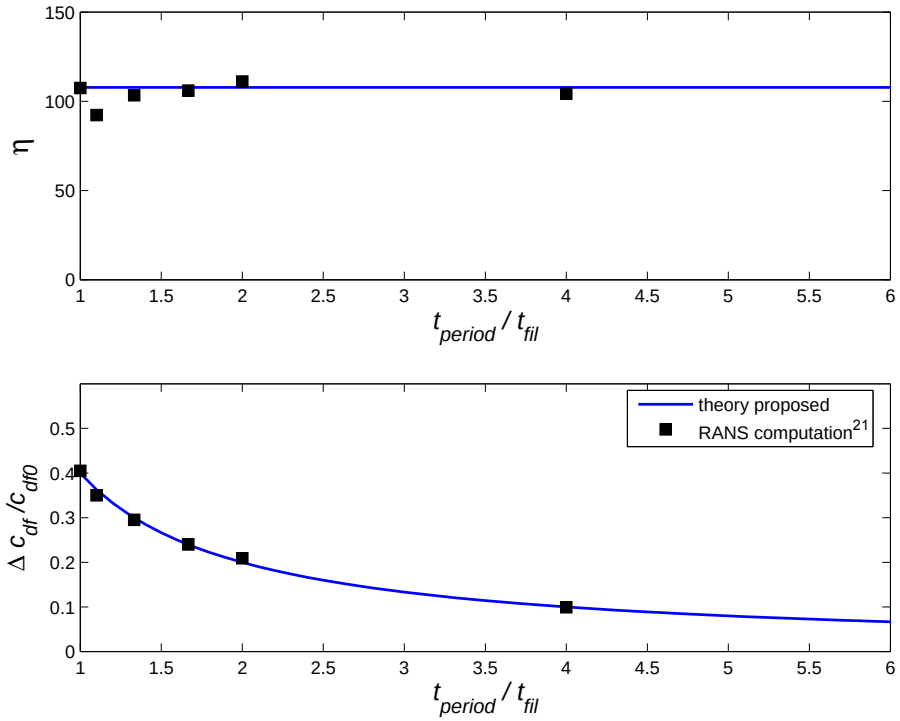

Figure 9. Effects of the periodic heating ratio t_{period}/t_{fil} on the efficiency η (top) and drag reduction ratio $\Delta c_{df}/c_{df0}$ (bottom) for the blunt cylinder body at $M_1 = 1.89$ and $\varepsilon = 1.0$, as obtained in Ref. 21

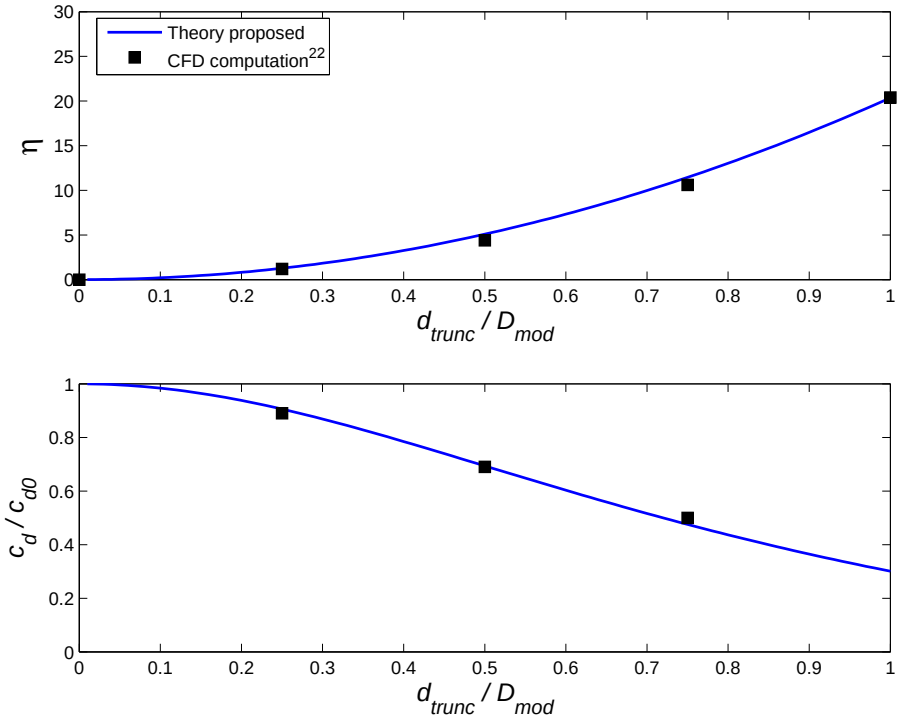

Figure 10. Average effect of the short-pulse flow heating for different truncated cones at Mach 2 for the case with an energy deposition of 3 mJ/pulse at 100 kHz introduced at the distance $x/d_{trunc} = 2.5$ upstream of the nose.[22]

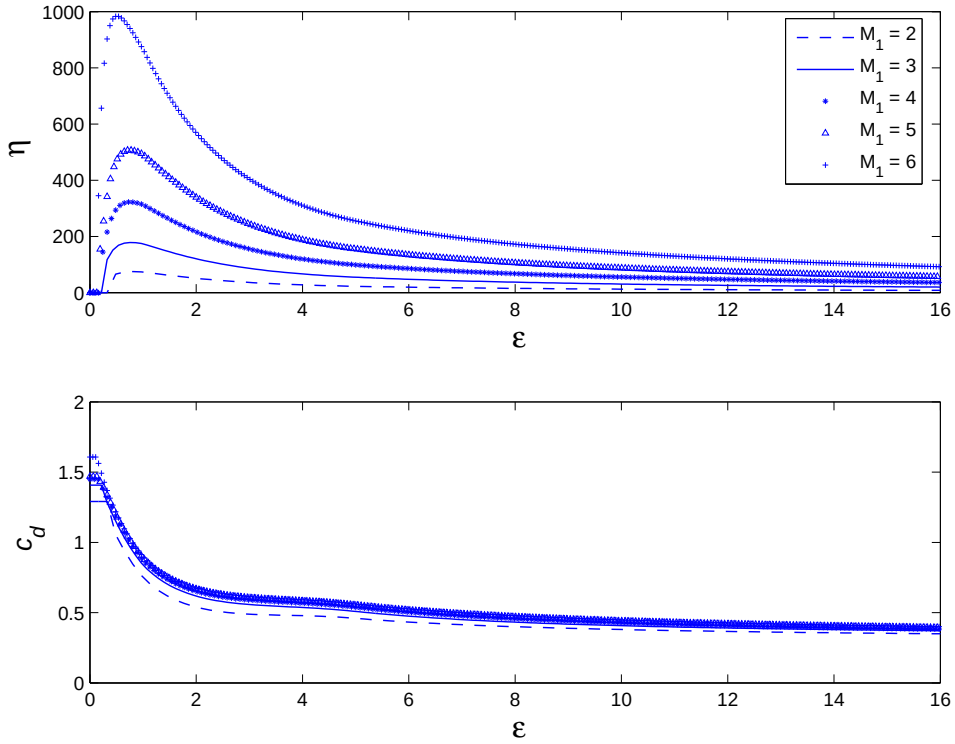

Figure 11. Effect of the freestream Mach number on the efficiency η (top) and drag coefficient c_d (bottom) predicted for a cone/cylinder body with $\theta_c = 55^\circ$.

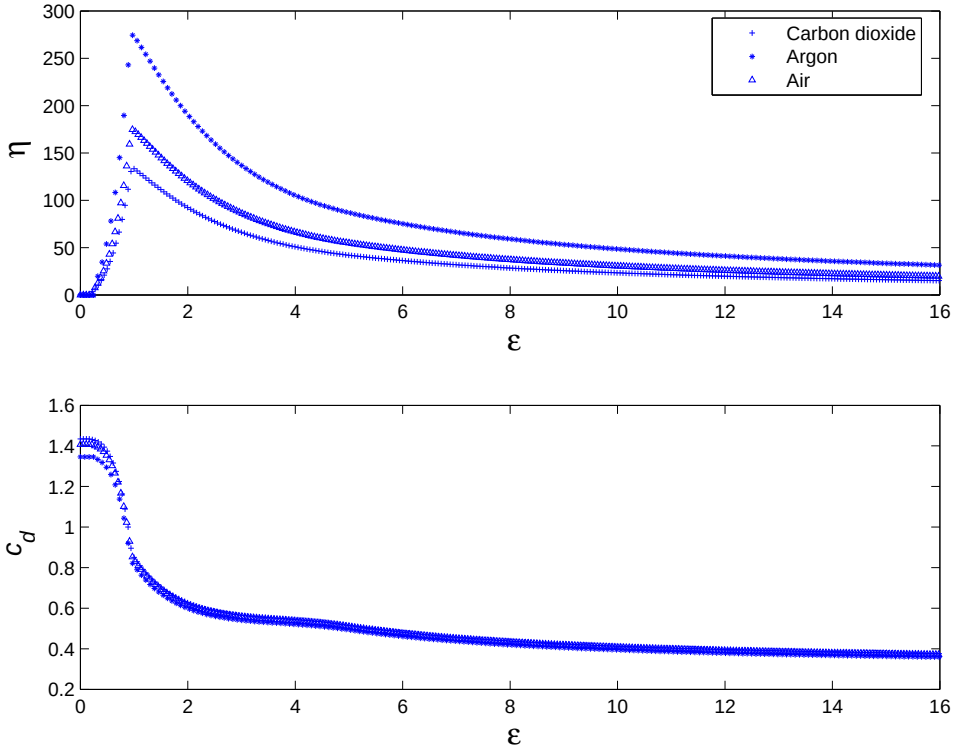

Figure 12. Effect of different gases on the efficiency η (top) and drag coefficient c_d (bottom) for a cone/cylinder body at $M_1 = 3$ and $\theta_c = 55^\circ$.

the aerodynamic performance of bodies with initially attached and detached bow-shock waves and seems to be robust and precise enough for desired parametric studies. The obtained results and the underlying model itself can help to advance the understanding of the processes behind the wave drag reduction effects of the energy deposition.

References

[1]Maurer, F., Brungs, W.: Beeinflussung des Widerstands und der Kopfwelle durch Wärmezufuhr im Staupunktsbereich stumpfer Körper bei Überschallanströmung. Jahrbuch 1968 der DGLR, Köln, 174-189, (1968) (in German)

[2]Georgievsky, P. Yu., Levin, V. A.: Supersonic Flow over Bodies in the Presence of External Energy Input Sources. Pisma v Zhurn. Tekhn. Phiz.,14(8), 684-687, (1988) (in Russian)

[3]Nemchinov, I.V., Artem'ev, V.I., Bergelson, V.I., Khazins, V.M., Orlova, T.I., Rybakov, V.A.: Rearrangement of the bow shock shape using a "hot spike". Shock Waves, 4(1), 35-40, (1994)

[4]Riggins, D., Nelson, H.F., Johnson, E.: Blunt-Body Wave Drag Reduction Using Focused Energy Deposition. AIAA J., 37(4), 460-467, (1999)

[5]Zheltovodov, A.A.: Development of the studies on energy deposition for application to the problems of supersonic aerodynamics. Preprint No. 10-2002, ITAM, RAS, SB, 43 p., Novosibirsk, (2002)

[6]Knight, D., Kuchinskiy, V., Kuranov, A., Sheikin, E.: Survey of aerodynamic flow control at high speed by energy deposition. AIAA-2003-0525, (2003)

[7]Norton, K., Knight, D.D.: Thermal Effects of Microwave Energy Deposition in Supersonic Flow. AIAA-2009-1224, (2009)

[8]Schülein, E., Zheltovodov, A.A.: Effects of localized flow heating by arc discharge upstream of non-slender bodies. Shock Waves, 21(4), 383-396, (2011)

[9]Schülein, E., Bornhöft, E.: Potential of Localized Flow Heating for Wave Drag Reduction. In: 28*th* International Symposium on Shock Waves Shock Waves, Vol. 1 (VIII), Springer, Heidelberg New York, 615-621, (2012)

[10]Oswatitsch, K.: Gasdynamik. Springer, Wien, 456 p., (1952) (in German)

[11]Vlasov, V.V., Grudnitskii, B.G., Rygalin, V.N.: Gas Dynamics with Local Energy Release in Supersonic and Subsonic Flow. Fluid Dynamics, 30(2), 275-280, (1995)

[12]Georgievsky, P. Yu., Levin, V. A.: Bow Shock Wave Structures Control by Pulse-Periodic Energy Input. AIAA-2004-1019, (2004)

[13]Liepmann, H.W., Roshko, A.: Elements of Gasdynamics. John Wiley & Sons, Inc., New York, London (1960)

[14]Moeckel, W.E.: Flow Separation Ahead of Blunt Bodies at Supersonic Speeds. NACA TN 2418, Washington, (1951)

[15]Guvernjuk, S., Savinov, K.: Isobaric Separation Structures in Supersonic Flows with a Localized Inhomogeneity. Doklady Physics, 52(3), 151-155, (2007)

[16]Georgievsky, P.Yu., Levin, V. A., Suturin, O.G.: Front Separation Regions Initiated by Upstream Energy Deposition. AIAA-2008-1355, (2008)

[17]Bornhöft, E.: Windkanaluntersuchungen zur Strömungssteuerung mittels Energiezufuhr. Master thesis, Univesität Göttingen & DLR Gttingen, (2010) (in German)

[18]Love, E.S., Woods, W.C., Rainey, R.W., Ashby, G.C.Jr.: Some Topics in Hypersonic Body Shaping. AIAA-1969-181, (1969)

[19]Knight, D.D., Zheltovodov, A.A.: Ideal-gas - shock wave turbulent boundary layer interactions in supersonic flows and their modeling: two-dimensional interactions. In: Shock Wave - Boundary Layer Interactions, Chapter 4, Edited by H.Babinsky & J.Harvey. Cambridge University Press (2011)

[20]Zheltovodov,A.A., Schülein, E.: Peculiarities of turbulent separation development in disturbed boundary layers. Modelirovanie v Mekhanike (Modeling in Mechanics), 2, 1, 53-8, (1988) (in Russian)

[21]Anderson, K., Knight, D.D.: Interaction of heated filaments with a blunt cylinder in supersonic flow. Shock Waves, 21:149-161, (2011)

[22]Sakai, T.: Supersonic Drag Performance of Truncated Cones with Repetitive Energy Depositions. International Journal of Aerospace Innovations, 1(1), 31-43, (2009)

[23]Satheesh, K., Jagadeesh, G.: Experimental Investigations of the Effect of Energy Deposition in Hypersonic Blunt Body Flow Field. Shock Waves, 18(1), 53-70, (2008)